On the BER Analysis of NOMA Systems

Arafat Al-Dweik, *Senior Member, IEEE*, Abla Bedoui, and Youssef Iraqi, *Senior Member, IEEE*

***Abstract*—The bit error rate (BER) analysis of non-orthogonal multiple access (NOMA) has been widely considered in the literature with the assumptions of perfect and imperfect successive interference cancellation (SIC). For both cases, exact closed-form formulas were derived under various channel models, number of users, and modulation orders. However, all the analysis reported overlooked the transformations that affect the probability density function (PDF) of additive white Gaussian noise (AWGN) after the SIC process. Therefore, the signal model after the SIC process is generally inaccurate, which makes the analysis just approximations rather than exact because the noise after SIC is not Gaussian anymore. Therefore, this letter derives the exact noise PDF after the SIC process and evaluates its impact on the BER analysis. The analytical results obtained show that the noise PDF after SIC should be modeled as a truncated Gaussian mixture. Moreover, the PDF after successful and unsuccessful SIC should be modeled differently.**

***Index Terms*—non-orthogonal multiple access (NOMA), probability density function (PDF), successive interference cancellation (SIC), truncated Gaussian, bit error rate (BER).**

I. Introduction

In recent years, the bit error rate (BER) analysis of non-orthogonal multiple access (NOMA) has received enormous attention from the research community, a comprehensive survey is given in [1]. The BER analysis is typically carried out assuming that the successive interference cancellation (SIC) process is perfect [2] or imperfect [3]–[6]. The case with perfect SIC is typically referred to as an approximation, while the case with imperfect SIC is typically referred to as exact. The same argument applies to other performance metrics such as outage probability, capacity, and signal-to-interference plus noise ratio (SINR).

The typical system model used in the literature for BER analysis of a two-user downlink power domain NOMA considers a base station (BS) that transmits two symbols, s_1 to the far-user (U_1), and s_2 to the near-user (U_2) [1], [4]–[9]. Therefore, the superposition NOMA signal can be written as

$$X = \sqrt{\alpha_1}s_1 + \sqrt{\alpha_2}s_2 \tag{1}$$

where α_1 and α_2 are the power allocation coefficients for U_1 and U_2, respectively, $\alpha_1 > \alpha_2$, and $\alpha_1 + \alpha_2 = 1$. To simplify the discussion in this letter, we consider binary phase shift keying (BPSK), therefore, $\{s_1, s_2\} \in \{-1, 1\}$, which are the modulated versions of the data bits $\{x_1, x_2\} \in \{0, 1\}$, $0 \rightarrow -1$, and $1 \rightarrow 1$.

The signal at U_2 receiver can be expressed as

$$y_2 = h_2(\sqrt{\alpha_1}s_1 + \sqrt{\alpha_2}s_2) + n \tag{2}$$

where h_2 is the channel fading coefficient between the BS and U_2 and $n \sim \mathcal{N}(0, \sigma_n^2)$ is an additive white Gaussian noise (AWGN). To detect its own symbol, U_2 must first detect s_1, apply SIC, and then detect s_2. Therefore, U_2 computes

$$\hat{s}_1 = \arg\min_{s_1} |y_2 - h_2\sqrt{\alpha_1}s_1|^2 . \tag{3}$$

Once $\hat{s}_1$ is obtained, SIC is applied such that $\tilde{y}_2 = y_2 - h_2\sqrt{\alpha_1}\hat{s}_1$, which gives

$$\tilde{y}_2 = h_2(\sqrt{\alpha_1}s_1 + \sqrt{\alpha_2}s_2 - \sqrt{\alpha_1}\hat{s}_1) + n. \tag{4}$$

Given that the SIC was successful, $\hat{s}_1 = s_1$, the SIC outcome becomes

$$\tilde{y}_2|_{\hat{s}_1=s_1} = h_2\sqrt{\alpha}_2 s_2 + n. \tag{5}$$

and finally,

$$\hat{s}_2 = \arg\min_{s_2} |\tilde{y}_2 - h_2\sqrt{\alpha_2}s_2|^2 . \tag{6}$$

The perfect SIC analysis is performed while assuming that $\hat{s}_1 = s_1$ regardless of the actual outcome of the SIC process. The estimated hard decision bits $\{\hat{x}_1, \hat{x}_2\}$ are obtained by demodulating the maximum likelihood detector (MLD) output $\{\hat{s}_1, \hat{s}_2\}$.

If the SIC fails, the outcome can be written as

$$\tilde{y}_2|_{\hat{s}_1\neq s_1} = h_2(\sqrt{\alpha_1}s_1 + \sqrt{\alpha_2}s_2 - \sqrt{\alpha_1}\hat{s}_1) + n,\ \hat{s}_1 \neq s_1. \tag{7}$$

It is usually assumed that the detector does not have information about the outcome of the SIC process, and hence, even if the SIC fails, $\tilde{y}_2$ in (4) is still applied to (6) to detect s_2, however, the probability of correctly detecting s_2 in this case is low. Furthermore, the error will also depend on the residual interference $\sqrt{\alpha_1}\hat{s}_1$, which is random because $\hat{s}_1$ is random.

The BER for U_2 using SIC can be expressed as

$$P_{B_2} = (P_{B_2}|_{\hat{s}_1=s_1})\Pr(\hat{s}_1 = s_1) + (P_{B_2}|_{\hat{s}_1\neq s_1})\Pr(\hat{s}_1 \neq s_1) \tag{8}$$

where $\Pr(\hat{s}_1 \neq s_1)$ is the probability of error for U_1 at U_2 [3]–[5]. At high signal-to-noise ratios (SNRs), $\Pr(\hat{s}_1 = s_1) \gg \Pr(\hat{s}_1 \neq s_1)$.

A. Motivation and Contribution

Although the mathematical formulation in (5) and (7) is widely adopted in the published literature, the formulation ignores the fact that noise in these cases should be written in a conditional form due to the dependence of the noise probability density function (PDF) on the SIC outcome, that is, it should be written as $n|_{\hat{s}_1=s_1} \triangleq w$ and $n|_{\hat{s}_1\neq s_1} \triangleq z$ for the successful and failed SIC, respectively. Based on an extensive literature search and to the best of the authors' knowledge, there is no prior work in the open literature that evaluates the impact of the SIC process on the AWGN in NOMA systems. Therefore, the objective of this letter is to derive the PDF of AWGN after successful and failed SIC, and to investigate its impact on the BER analysis. The contribution of this letter can be summarized as follows:

- Derive the exact PDF of the AWGN after the SIC process. The analytical results obtained corroborated by simula-

A. Al-Dweik is with the 6G Research Center, Department of Computer and Communications Engineering, Khalifa University, Abu Dhabi, UAE. (e-mail: arafat.dweik@ku.ac.ae, dweik@fulbrightmail.org).

A. Bedoui and Y. Iraqi are with the College of Computing, University Mohammed IV Polytechnic, Bengurir, Morocco. (e-mails: {abla.bedoui, youssef.iraqi}@um6p.ma)

Manuscript received December, 2023; revised —- –, —-.

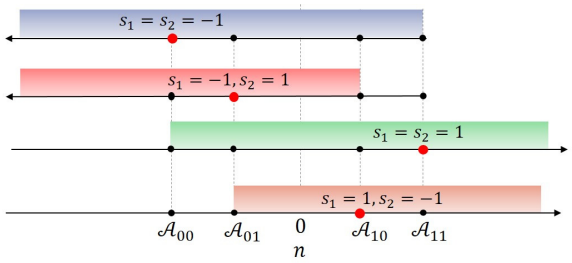

(a) The SIC is successful $\hat{s}_1 = s_1$.

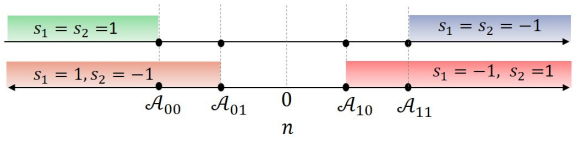

(b) The SIC fails $\hat{s}_1 \neq s_1$.

Fig. 1: Illustration of the noise regions for successful and unsuccessful SIC.

tion show that the conditional noise PDF is drastically different from the original Gaussian PDF before SIC

- Evaluate the impact of the SIC process on the apriori probabilities of the NOMA symbols. The obtained results show that NOMA symbols probabilities become nonuniform after SIC even though the apriori probabilities of the NOMA symbols are uniform.
- Derive the exact BER after a successful SIC and evaluate the difference with respect to the Gaussian model. The derived analysis shows that the BER formula of the widely used perfect SIC model using AWGN is actually an approximation rather than an exact as typically considered by the research community.

B. Paper Organization

The rest of the letter is organized as follows. Sec. II derives the PDF of the noise after SIC. The BER is derived in Sec. III, and finally, Sec. IV concludes the letter.

II. PDF of the AWGN after SIC

To derive the noise PDF after SIC, we need to identify the noise values that cause successful and unsuccessful SIC. Fig. 1a shows the regions for n when the SIC is successful for each transmitted NOMA symbol. The NOMA symbols and amplitudes are defined in Table I. The amplitudes A_{ij} are defined such that $i \in \{0,1\}$ is associated with the value of bit x_1 while $j \in \{0,1\}$ is associated with the value of bit x_2, and $\mathcal{A}_{ij} = |h_2|A_{ij}$. The noise range that leads to a successful SIC can be obtained by finding the threshold at which s_1 will be detected successfully. For BPSK, the MLD of U_1 can be written as $y_2 \underset{-1}{\overset{1}{\gtrless}} 0$. Based on Fig. 1a and Table I, the noise range given that $s_1 = 1$ will be such that $n \in (-\mathcal{A}_{1j}, \infty]$, or equivalently $n \in (\mathcal{A}_{0\bar{j}}, \infty]$, where $\bar{j}$ is the inverted j, i.e., $\bar{0} = 1$ and $\bar{1} = 0$. Similarly, for $s_1 = -1$, the noise range will be $n \in [-\infty, -\mathcal{A}_{0j})$, which can be written as $n \in [-\infty, \mathcal{A}_{1\bar{j}})$. For example, for $[s_1 = 1, s_2 = -1]$, a successful SIC, $\hat{s}_1 = 1$, occurs if $n \in [\mathcal{A}_{01}, \infty]$. For $[s_1 = -1, s_2 = 1]$, successful SIC, $\hat{s}_1 = -1$, occurs when $n \in [-\infty, \mathcal{A}_{10}]$. The same approach can be applied to identify the noise regions that cause an unsuccessful SIC, which are shown in Fig. 1b.

When a normally distributed random variable is constrained to specific intervals, it undergoes a transformation into a truncated Gaussian distribution [10]. This distribution is formally denoted as $\mathcal{F}(n; \mu, \sigma^2, [a_1, b_1], [a_2, b_2], \dots)$, where μ and σ are the mean and variance of the parent Gaussian distribution, respectively. It is worth noting that the moments of the truncated Gaussian distribution, such as mean and variance, can be easily derived in terms of their counterparts in the Gaussian distribution [11]. The truncated Gaussian PDF over the intervals $[a_1, b_1], [a_2, b_2], \dots, [a_L, b_L]$ can be computed as

$$f(n|_{[a_1 \le n \le b_1], \dots, [a_L \le n \le b_L]}) = \frac{\sum_{i=1}^{L} I_{[a_i, b_i]}(n)}{\sum_{i=1}^{L} \int_{a_i}^{b_i} f_N(n) dn} f_N(n) \tag{9}$$

where the indicator function $I_{[a,b]}(n) = 1$ for $n \in [a, b]$, and 0 otherwise, and $n \sim \mathcal{N}(0, \sigma_n^2)$ is the parent AWGN PDF,

$$f_N(n) = \frac{1}{\sqrt{2\pi\sigma_n^2}} \exp\left(-\frac{n^2}{2\sigma_n^2}\right). \tag{10}$$

Considering the different intervals in Fig. 1a, the PDF of the noise after a successful SIC is a truncated Gaussian mixture that can be computed as

$$\begin{aligned} f_W(w) &= f_W(w|_{s_1=-1}) \Pr(s_1 = -1) \\ &\quad + f_W(w|_{s_1=1}) \Pr(s_1 = 1) \\ &= \frac{1}{2}(f_W(w|_{s_1=-1}) + f_W(w|_{s_1=1})) \end{aligned} \tag{11}$$

where $\Pr(s_1 = -1) = \Pr(s_1 = 1) = 0.5$, and

$$f_W(w|_{s_1=-1}) = \frac{\Phi(-w + \mathcal{A}_{11}) + \Phi(-w + \mathcal{A}_{10})}{\int_{-\infty}^{\mathcal{A}_{11}} f_N(w)\, dw + \int_{-\infty}^{\mathcal{A}_{10}} f_N(w)\, dw} f_N(w) \tag{12}$$

$$f_W(w|_{s_1=1}) = \frac{\Phi(w - \mathcal{A}_{00}) + \Phi(w - \mathcal{A}_{01})}{\int_{\mathcal{A}_{00}}^{\infty} f_N(w)\, dw + \int_{\mathcal{A}_{01}}^{\infty} f_N(w)\, dw} f_N(w) \tag{13}$$

$\Phi(\cdot)$ is the Heaviside step function. The integrals in (12) and (13) can be evaluated as

$$\int_{-\infty}^{a} f_N(w)\, dw = \frac{1}{2}\left(1 + \operatorname{erf}\left(\frac{a}{\sigma_n\sqrt{2}}\right)\right) \tag{14}$$

and $\int_a^{\infty} f_N(w)\, dw = 1 - \int_{-\infty}^{a} f_N(w)\, dw$, $\operatorname{erf}(\cdot)$ is the Gauss error function.

The same approach is used to derive $f(z)$ for the unsuccessful SIC scenario,

$$f_Z(z) = \frac{1}{2}\left(f_Z(z|_{s_1=-1}) + f_Z(z|_{s_1=1})\right) \tag{15}$$

where

$$f_Z(z|_{s_1=-1}) = \frac{\Phi(z - \mathcal{A}_{11}) + \Phi(z - \mathcal{A}_{10})}{\int_{\mathcal{A}_{11}}^{\infty} f_N(z)\, dz + \int_{\mathcal{A}_{10}}^{\infty} f_N(z)\, dz} f_N(z) \tag{16}$$

$$f_Z(z|_{s_1=1}) = \frac{\Phi(-z + \mathcal{A}_{00}) + \Phi(-z + \mathcal{A}_{01})}{\int_{-\infty}^{\mathcal{A}_{00}} f_N(z)\, dz + \int_{-\infty}^{\mathcal{A}_{01}} f_N(z)\, dz} f_N(z). \tag{17}$$

The derived truncated Gaussian PDFs after the SIC process are shown in Figs. 2 and 3 where $|h_2| = 1$. For the case of SNR= 0 dB in Fig. 2, the difference between the Gaussian and the truncated PDFs for the successful and unsuccessful SIC cases is significant, particularly in the center of the PDF. For SNR of 10 dB in Fig. 3, it can be seen that $f_W(w) \sim f_N(n)$,

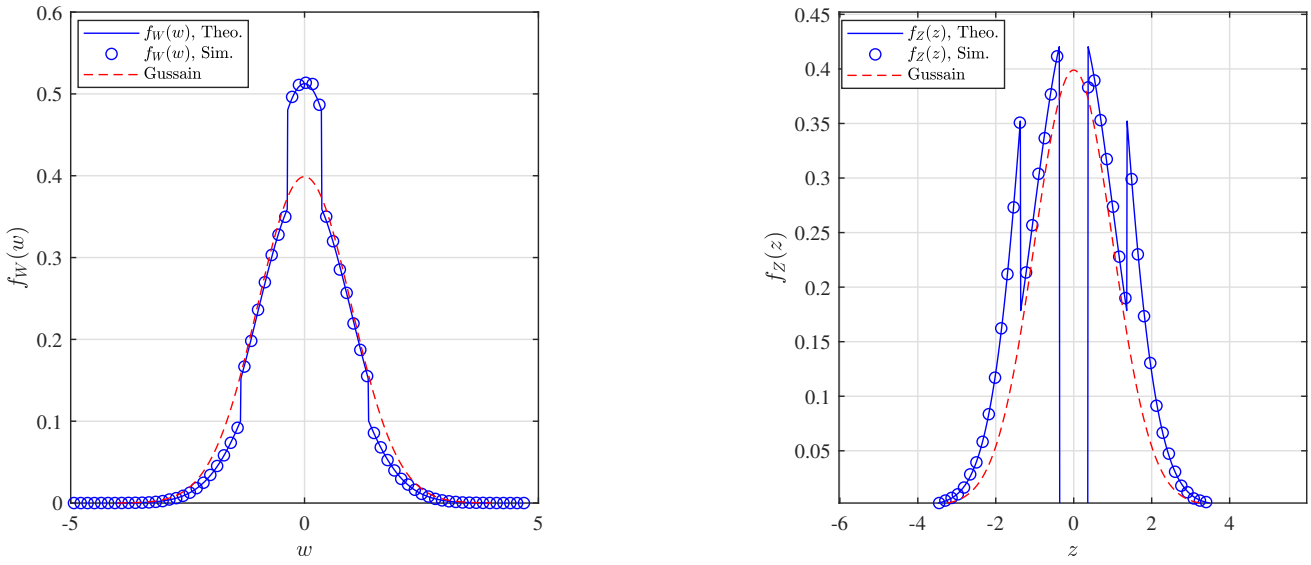

(a) $f_W(w)$ (b) $f_Z(z)$

Fig. 2: PDF of the AWGN before and after successful and unsuccessful SIC, $\alpha_1 = 0.75$, $\alpha_2 = 0.25$, SNR= 0 dB.

TABLE I: NOMA transmitted (Tx) and received (Rx) constellation (Const.) points notation, For U_2, $\mathcal{A}_{ij} = |h_2|A_{ij}$.

x_1	s_1	x_2	s_2	Tx Const.	Rx Const.
0	−1	0	−1	$A_{00} = -\sqrt{\alpha_1} - \sqrt{\alpha_2}$	$\mathcal{A}_{00}$
0	−1	1	1	$A_{01} = -\sqrt{\alpha_1} + \sqrt{\alpha_2}$	$\mathcal{A}_{01}$
1	1	0	−1	$A_{10} = \sqrt{\alpha_1} - \sqrt{\alpha_2}$	$\mathcal{A}_{10}$
1	1	1	1	$A_{11} = \sqrt{\alpha_1} + \sqrt{\alpha_2}$	$\mathcal{A}_{11}$

while the difference is significant for $f_Z(z)$. Therefore, the exact BER for the near-user should be re-derived using the truncated PDF instead of the regular Gaussian PDFs. Consequently, the BER derived in the literature for the perfect SIC is actually an approximation rather than an exact.

III. Bit Error Rate Analysis

To demonstrate the effect of the noise distribution on the BER, we consider the widely used perfect SIC assumption. Therefore, the BER of U_2 can be computed as

$$P_{B_2} = \sum_{i=0}^{1}\sum_{j=0}^{1}(P_{B_2}|\tilde{A}_{ij})\Pr(\tilde{A}_{ij}) \tag{18}$$

where $\tilde{A}_{ij}$ represents the probability that constellation point A_{ij} is transmitted given that $\hat{s}_1 = s_1$, i.e., $\Pr(\tilde{A}_{ij}) = \Pr(A_{ij}|\hat{s}_1 = s_1)$. Using Bayes' Theorem we obtain

$$\Pr(A_{ij}|\hat{s}_1 = s_1) = \frac{\Pr(\hat{s}_1 = s_1|A_{ij})\Pr(A_{ij})}{\Pr(\hat{s}_1 = s_1)}. \tag{19}$$

The case of $\tilde{A}_{00}$ can be computed as

$$\begin{aligned}\Pr(\tilde{A}_{00}) &= \frac{\left[1 - \int_{\mathcal{A}_{11}}^{\infty} f_N(n)\,dn\right]\Pr(A_{00})}{1 - \frac{1}{2}\left[\int_{\mathcal{A}_{11}}^{\infty} f_N(n)\,dn + \int_{\mathcal{A}_{10}}^{\infty} f_N(n)\,dn\right]} \\ &= \frac{1 + \mathrm{erf}\left(\sqrt{\frac{\Omega}{2}}\mathcal{A}_{11}\right)}{4 + 2\mathrm{erf}\left(\sqrt{\frac{\Omega}{2}}\mathcal{A}_{11}\right) + 2\mathrm{erf}\left(\mathcal{A}_{10}\sqrt{\frac{\Omega}{2}}\right)},\end{aligned} \tag{20}$$

where $\Omega = \frac{1}{\sigma_n^2} \triangleq \mathrm{SNR}$. The remaining cases can be computed as $\Pr(\tilde{A}_{00}) = \Pr(\tilde{A}_{11})$, $\Pr(\tilde{A}_{01}) = \Pr(\tilde{A}_{10}) = \frac{1}{2} - \Pr(\tilde{A}_{00})$. By noting that

$$P_{B_2}|A_{00} = P_{B_2}|A_{11} = \int_{|h_2|\sqrt{\alpha_2}}^{\mathcal{A}_{11}} f_W(w|A_{00})\,dw \tag{21}$$

$$P_{B_2}|A_{01} = P_{B_2}|A_{10} = \int_{-\infty}^{-|h_2|\sqrt{\alpha_2}} f_W(w|A_{01})\,dw \tag{22}$$

$$f_W(w|A_{0j}) = \frac{2\Phi(-w + \mathcal{A}_{1\bar{j}})}{1 + \mathrm{erf}\left(\sqrt{\frac{\Omega}{2}}\mathcal{A}_{1\bar{j}}\right)} f_N(w) \tag{23}$$

$$f_W(w|A_{1j}) = \frac{2\Phi(w - \mathcal{A}_{0\bar{j}})}{1 - \mathrm{erf}\left(\sqrt{\frac{\Omega}{2}}\mathcal{A}_{0\bar{j}}\right)} f_N(w). \tag{24}$$

Then, by substituting the expressions of $P_{B_2}|\tilde{A}_{ij}$ and $\Pr(\tilde{A}_{ij})$ $\forall\{i,j\}$ into (18), evaluating the integrals, and performing some manipulations, we obtain

$$P_{B_2} = \frac{2\mathrm{erf}\left(|h_2|\sqrt{\alpha_2\frac{\Omega}{2}}\right) + \mathrm{erf}\left(\sqrt{\frac{\Omega}{2}}\mathcal{A}_{00}\right) - 1}{\mathrm{erf}\left(\sqrt{\frac{\Omega}{2}}\mathcal{A}_{00}\right) + \mathrm{erf}\left(\sqrt{\frac{\Omega}{2}}\mathcal{A}_{01}\right) - 2}. \tag{25}$$

For the perfect SIC with AWGN, P_{B_2} is equivalent to the BER of orthogonal multiple access (OMA) with BPSK, which is given by

$$P_{B_2} = \frac{1}{2}\left[1 - \mathrm{erf}\left(\sqrt{\frac{\alpha_2|h_2|^2\Omega}{2}}\right)\right]. \tag{26}$$

Therefore, the difference between the two cases is apparent. In particular, it can be seen in (25) that the denominator has an $\mathrm{erf}(\cdot)$ function, which makes averaging over PDF of $|h_2|$ or α_2 intractable. The BER expression in (26) is denoted as legacy BER.

Fig. 4 shows the legacy BER (26) and conditional $P_{B_2}|_{X=A_{00}}$ and $P_{B_2}|_{X=A_{01}}$ for $|h_2| = 1$ and 0.1. As can be

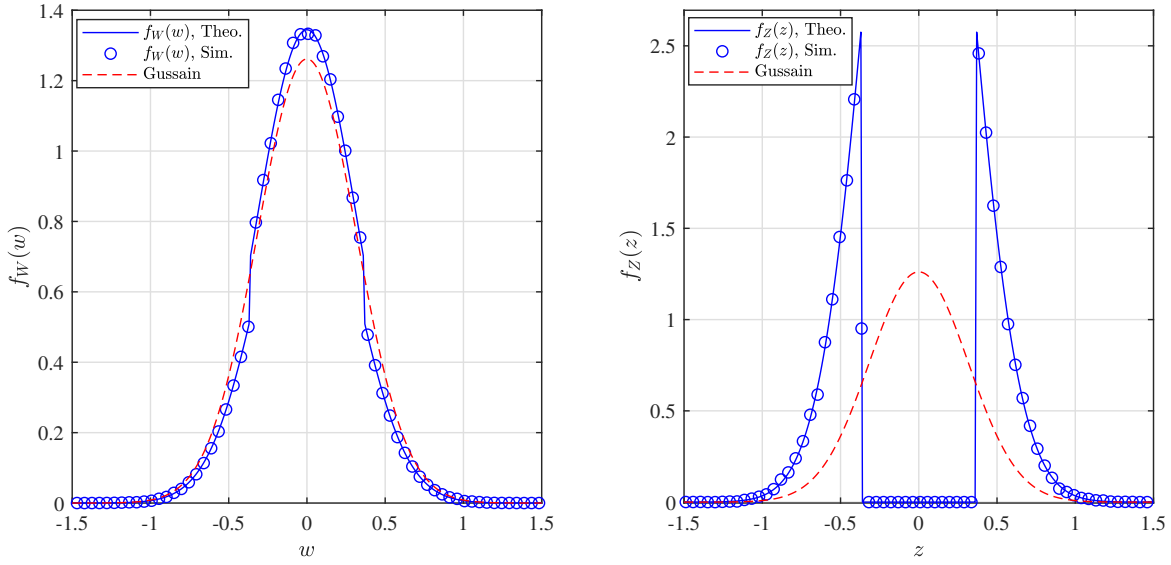

(a) $f_W(w)$ (b) $f_Z(z)$

Fig. 3: PDF of the AWGN before and after successful and unsuccessful SIC, $\alpha_1 = 0.75$, $\alpha_2 = 0.25$, SNR= 10 dB.

seen from Fig. 4a, the BER difference is more significant at low SNRs and $P_{B_2}|_{X=A_{00}} < P_{B_2}|_{X=A_{01}}$. The same behavior is observed in Fig. 4b, but $P_{B_2}|_{X=A_{00}} \ll P_{B_2}|_{X=A_{01}}$. It can also be seen that $P_{B_2}|_{X=A_{00}}$ increases versus SNR$\in \{0, 20\}$ dB, which is due to the noise truncation process. As expected, the legacy BER is independent of X and is bounded by $P_{B_2}|_{X=A_{00}}$ and $P_{B_2}|_{X=A_{01}}$.

Fig. 5 shows the average BER of the new and legacy BER, which is obtained using (26), which corresponds to the exact BER while assuming perfect SIC and AWGN. As can be seen in the figure, the BER difference is inversely proportional to α_1 and to SNR. For $\alpha_1 = 0.7$, the error becomes negligible at moderate and high SNRs while it is not the case for $\alpha_1 = 0.55$. Generally speaking, the difference between the new and legacy average BER is not as large as the case of conditional BER in Fig. 4. Such a performance is obtained because the average of $P_{B_2}|_{X=A_{00}}$ and $P_{B_2}|_{X=A_{01}}$ generally approaches the legacy BER.

Fig. 6 further illustrates the relation between the new and the legacy BERs by computing the ratio of the legacy to the new BER. As can be seen in the figure, the ratio is bounded between 0.5 and 1 where it converges to 1 at low SNRs, while it converges to 0.5 at high SNRs. It can also be seen that the convergence rate is proportional to $|h_2|$. For example, when $|h_2| = 4$, the ratio approaches 0.5 at ≈ 0 dB. For a given $|h_2|$, the impact of α_1 decreases at low and high SNRs, however, the difference is generally less than 4% for any scenario.

IV. Conclusion

This letter discussed the exact PDFs of the Gaussian noise after the SIC process in NOMA receivers. The results obtained showed that the PDF of AWGN undergoes a significant transformation after the SIC process, which has been overlooked in the published literature. More specifically, the AWGN is transformed into a truncated-Gaussian mixture, and the PDFs after successful and unsuccessful SIC are different. The BER

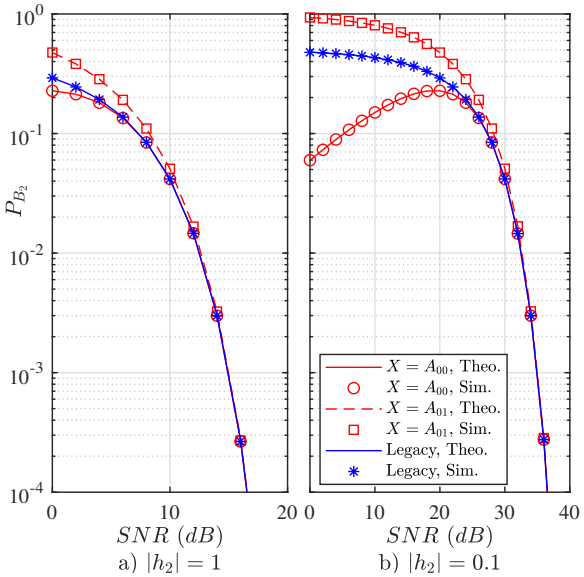

Fig. 4: The conditional BER given that $X = A_{00}$ and $X = A_{01}$.

analysis showed that the difference between the new and legacy analysis is generally small, and therefore the difference between the simulation and legacy BER did not trigger any inquiry on the correctness of the legacy analysis.

In future work, it will be crucial to evaluate the various performance metrics of NOMA, such as BER, capacity, SINR, and outage, using the new derived noise PDFs. Moreover, the analysis can be extended to consider various channel and system settings.

References

[1] H. Yahya, A. Ahmed, E. Alsusa, A. Al-Dweik, and Z. Ding, "Error rate analysis of NOMA: Principles, survey and future directions," *IEEE Open J. Commun. Soc.*, vol. 4, pp. 1682–1727, 2023.

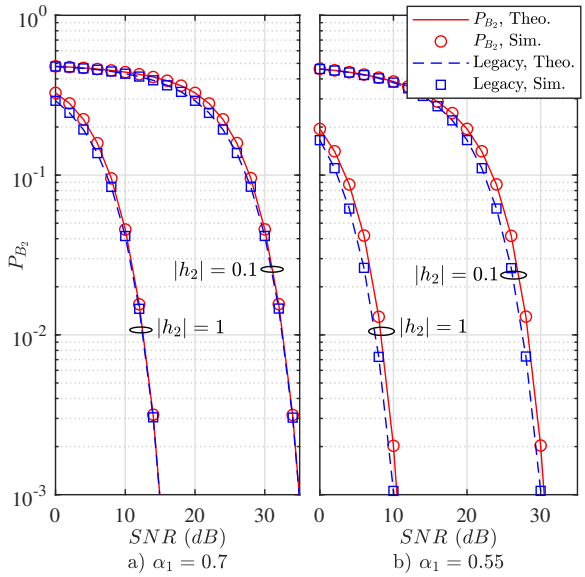

Fig. 5: BER using the exact and Gaussian noise PDF (legacy) for the perfect SIC scenario.

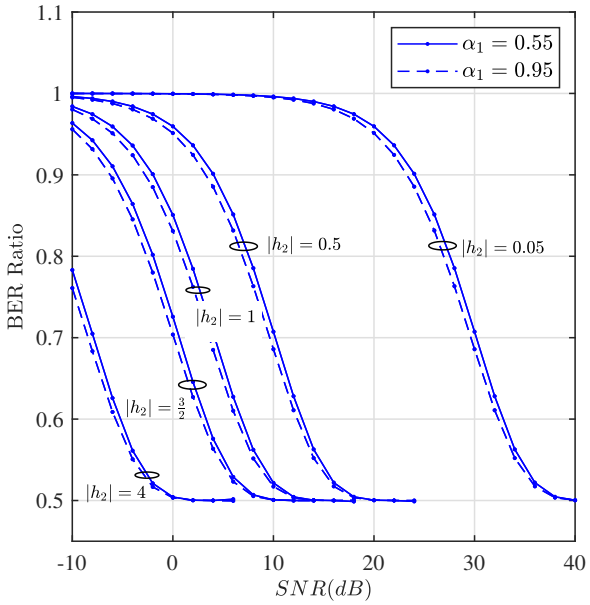

Fig. 6: The ratio of the legacy BER (26) to the new-exact BER (25) for various values of $|h_2|$, $\alpha_1 \in \{0.55, 0.95\}$.

[2] M. Aldababsa, C. Göztepe, G. K. Kurt, and O. Kucur, "Bit error rate for NOMA network," *IEEE Commun. Lett.*, vol. 24, no. 6, pp. 1188–1191, 2020.
[3] L. Bariah, S. Muhaidat, and A. Al-Dweik, "Error performance of NOMA-based cognitive radio networks with partial relay selection and interference power constraints," *IEEE Trans. Commun.*, vol. 68, no. 2, pp. 765–777, 2020.
[4] H. Yahya, E. Alsusa, and A. Al-Dweik, "Exact BER analysis of NOMA with arbitrary number of users and modulation orders," *IEEE Trans. Commun.*, vol. 69, no. 9, pp. 6330–6344, 2021.
[5] Y. Zhang, J. Wang, L. Zhang, Y. Zhang, Q. Li, and K.-C. Chen, "Reliable transmission for NOMA systems with randomly deployed receivers," *IEEE Trans. Commun.*, vol. 71, no. 2, pp. 1179–1192, 2023.
[6] T. Assaf *et al.*, "Exact bit error-rate analysis of two-user NOMA using QAM with arbitrary modulation orders," *IEEE Commun. Lett.*, vol. 24, no. 12, pp. 2705–2709, 2020.
[7] M. Jain, N. Sharma, A. Gupta, D. Rawal, and P. Garg, "Performance analysis of NOMA assisted underwater visible light communication system," *IEEE Wireless Commun.*, vol. 9, no. 8, pp. 1291–1294, 2020.
[8] H. Semira, F. Kara, H. Kaya, and H. Yanikomeroglu, "Multi-user joint maximum-likelihood detection in uplink NOMA-IoT networks: Removing the error floor," *IEEE Wireless Commun. Lett.*, vol. 10, no. 11, pp. 2459–2463, 2021.
[9] C. Ouyang, Y. Liu, and H. Yang, "Revealing the impact of SIC in NOMA-ISAC," *IEEE Wireless Commun. Lett.*, vol. 12, no. 10, pp. 1707–1711, Oct. 2023.
[10] A. Papoulis, *Probability, random variables, and stochastic processes*. McGraw-Hill 3rd ed, 1991.
[11] A. C. Cohen, "On estimating the mean and standard deviation of truncated normal distributions," *J. of the American Statistical Association*, vol. 44, no. 248, pp. 518–525, 1949.